Journal of Inorganic Biochemistry 235 (2022) 111915

Contents lists available at ScienceDirect

Journal of Inorganic Biochemistry

journal homepage: www.elsevier.com/locate/jinorgbio

Decavanadate and metformin-decavanadate effects in human melanoma cells

Ana Luísa De Sousa-Coelho [a,b,c,1,*], Manuel Aureliano [d,e,**,1,2], Gil Fraqueza [e,f], Gisela Serrão [a], João Gonçalves [g], Irma Sánchez-Lombardo [h], Wolfgang Link [i,2], Bibiana I. Ferreira [a,b,g,2]

[a] Algarve Biomedical Center Research Institute (ABC-RI), Universidade do Algarve, Faro, Portugal
[b] Algarve Biomedical Center (ABC), Faro, Portugal
[c] Escola Superior de Saúde (ESS), Universidade do Algarve, Faro, Portugal
[d] Faculdade de Ciências e Tecnologia (FCT), Universidade do Algarve, Faro, Portugal
[e] Centro de Ciências do Mar (CCMar), Universidade do Algarve, Faro, Portugal
[f] Instituto Superior de Engenharia (ISE), Universidade do Algarve, Faro, Portugal
[g] Faculdade de Medicina e Ciências Biomédicas, Universidade do Algarve, Faro, Portugal
[h] División Académica de Ciencias Básicas, Universidad Juárez Autónoma de Tabasco, Cunduacán, Mexico
[i] Instituto de Investigaciones Biomédicas "Alberto Sols" (CSIC-UAM). Madrid, Spain

ARTICLE INFO

Keywords:
Decavanadate
Metformin
Metformin-decavanadate
Polyoxometalates
Polyoxovanadates
Skin cancer
Melanoma
Cell signaling

ABSTRACT

Decavanadate is a polyoxometalate (POMs) that has shown extensive biological activities, including antidiabetic and anticancer activity. Importantly, vanadium-based compounds as well as antidiabetic biguanide drugs, such as metformin, have shown to exert therapeutic effects in melanoma. A combination of these agents, the metformin-decavanadate complex, was also recognized for its antidiabetic effects and recently described as a better treatment than the monotherapy with metformin enabling lower dosage in rodent models of diabetes. Herein, we compare the effects of decavanadate and metformin-decavanadate on Ca^{2+}-ATPase activity in sarcoplasmic reticulum vesicles from rabbit skeletal muscles and on cell signaling events and viability in human melanoma cells. We show that unlike the decavanadate-mediated non-competitive mechanism, metformin-decavanadate inhibits Ca^{2+}-ATPase by a mixed-type competitive–non-competitive inhibition with an IC_{50} value about 6 times higher (87 μM) than the previously described for decavanadate (15 μM). We also found that both decavanadate and metformin-decavanadate exert antiproliferative effects on melanoma cells at 10 times lower concentrations than monomeric vanadate. Western blot analysis revealed that both, decavanadate and metformin-decavanadate increased phosphorylation of extracellular signal-regulated kinase (ERK) and serine/threonine protein kinase AKT signaling proteins upon 24 h drug exposure, suggesting that the anti-proliferative activities of these compounds act independent of growth-factor signaling pathways.

1. Introduction

In recent years, there is an increasing interest for the potential use of metals in health, including lithium (Li), tungstate (W), gold (Au) or vanadium (V), with different conceivable applications [1–4]. Besides the well-characterized platinum drugs, such metal-based complexes, namely gold compounds and/or polyoxotungstates (POTs), have shown potential activity against several cancers, showing inhibition of cancer cells proliferation by inhibiting mitochondrial enzyme activity and the induction of apoptosis [5–7]. Polyoxometalates (POMs), which are a diverse family of metal-oxo anions of early transitional metal ions (Mo, W, V), are gaining increasing interest in biomedicine due to their anti-cancer activities [8]. Recently, the anti-cancer potential of dozens of previously considered non oncologic drugs, such as specific vanadium (V)-containing drugs, was uncovered [9]. These results strengthened our hypothesis that metal-based complexes are potential novel treatments,

* Correspondence to: A.L. De Sousa-Coelho, Algarve Biomedical Center Research Institute (ABC-RI), Universidade do Algarve, Faro, Portugal.
** Correspondence to: M. Aureliano, Faculdade de Ciências e Tecnologia (FCT), Universidade do Algarve, Faro, Portugal.
E-mail addresses: alcoelho@ualg.pt (A.L. De Sousa-Coelho), maalves@ualg.pt (M. Aureliano).
[1] These authors have contributed equally to this work.
[2] These authors share senior authorship.

https://doi.org/10.1016/j.jinorgbio.2022.111915
Received 29 March 2022; Received in revised form 21 June 2022; Accepted 3 July 2022
Available online 8 July 2022

leading to great interest in better understanding the involved effectors and their mechanism of action in cancer cell biology. Mechanistically, a wide range of such uses in medicine may include the modulation several enzymes such as P-type ATPases activity [7,10–13], although many others targets have been proposed and reviewed for polyoxometalates and recently for polyoxovanadates [6,8,14,15]. In fact, POMs in cancer therapy and diagnostics, their modes of action, protein targets and future perspectives were recently reviewed [14–17]. The isopolyoxovanadate decavanadate (V_{10}) is perhaps the most widely studied of the POMs, demonstrating many important roles in fundamental biological processes [14,15,17–22]. Here we explore the therapeutic potential of decavanadate (V_{10}) and metformin-decavanadate (Metf-V_{10}) in melanoma, the most aggressive type of skin cancer. The incidence of melanoma has been increasing annually worldwide at a faster rate compared to any other type of malignant tumor [23]. Despite the inclusion of immunotherapy with remarkable clinical efficacy in the treatment of melanoma [24], relapse and development of therapy resistance is still a major hurdle to overcome [25]. Thus, the discovery of novel anti-cancer agents capable of overcoming drug resistance and sensitizing highly resistant cancer cells to therapy is paramount to improve current clinical outcomes. Over the last decade, different vanadium-based compounds have shown to have anti-cancer potential in melanoma, including oxidovanadium(IV) species, vanadium pentoxide, and inorganic ion vanadate [26–30], as recently reviewed [31]. The anti-cancer potential of vanadate complexes was also evidenced in other types of cancer, such as prostate, thyroid, esophageal squamous, and oral squamous cell carcinomas [32–36]. On the other hand, the oral anti-diabetic, biguanide drug metformin (Metf), has been considered a potential cancer therapy in melanoma, partially due to its inhibition of oxidative phosphorylation altering tumor metabolism [37]. Metformin-decavanadate (Metf-V_{10}) is a very interesting hybrid compound [38]. Metf-V_{10} has previously shown *in vivo* nontoxicological effects on liver and kidney, being overall considered a better treatment (in lower dosage) than the monotherapy with Metf in diabetes, as both insulin-mimetic and insulin-enhancing agent [39]. Aimed as a novel potential metallopharmaceutical [40,41], *in vivo* studies have described a relevant hypoglycemic action of Metf-V_{10} in rodent models of hypercaloric diet-induced insulin resistance and type 1 diabetes [39,42], though its biological effects in melanoma have never been studied. In this work, we have studied the the anti-cancer potential of vanadate-hybrid POMs compounds. We compared the effects of V_{10} and Metf-V_{10} in: 1) Ca^{2+}-ATPase activity; and 2) cellular proliferation, as well as mitogen-activated protein kinase / extracellular signal-regulated kinase (MAPK/ERK) and phosphoinositide 3-kinase / serine/threonine protein kinase (PI3K/AKT) signaling pathways, in human melanoma UACC-62 cells.

2. Materials and methods

2.1. Preparation of decavanadate and metformin-decavanadate

Ammonium metavanadate (99.9% NH_4VO_3) was purchased from Sigma-Aldrich. Pale yellow stock solutions of ammonium metavanadate (50 mM) were prepared in water after solubilization. The pH of this solution was adjusted with NaOH to 10.5 and heated until a colorless solution was obtained, *i.e.* the solution of monomeric vanadate (V_1). To obtain a solution of decavanadate (V_{10}), after cooling the solution of V_1, HCl was added until pH 4.0, resulting in a yellowish-orange colored solution of decavanadate with 5 mM concentration. Metformin-decavanadate (Metf-V_{10}) is composed of the negatively charged decavanadate ($[V_{10}O_{28}]^{6-}$) and the positive counter ion metformin (metforminium cation, $[C_4H_{12}N_5]^+$), with a 3:1 ratio of cation-anion ($[H_2Metf]_3[V_{10}O_{28}]\cdot 8H2O$). Metf-$V_{10}$ was synthesized according to published procedures [40]. The Metf-V_{10} crystals were solubilized in 10% dimethyl sulfoxide (DMSO) to a 5 mM stock concentration. Such vanadium compounds were previously characterized [40,43–45].

2.2. Preparation of sarcoplasmic reticulum Ca^{2+}-ATPase vesicles

Sarcoplasmic reticulum (SR) vesicles were prepared from rabbit skeletal muscles as described elsewhere [7,13,44,46]. SR vesicles (SRV) were suspended in 0.1 M KCl, 10 mM 2-[4-(2-hydroxyethyl)piperazin-1-yl]ethanesulfonic acid (HEPES, pH 7.0), diluted 1:1 with 2.0 M sucrose, and then immediately frozen in liquid nitrogen before storage at −80 °C until used. SRV total protein concentration was determined spectrophotometrically at 595 nm in the presence of 0.125% of sodium dodecyl sulphate (SDS) by the Bradford method [47]. Bovine serum albumin (BSA) was used as a standard. The proteins present in the SRV preparations were determined by densitometry analysis of the bands in a 7.5% acrylamide SDS-PAGE gel. The SR Ca^{2+}-ATPase constituted at least 70% of the total protein amount, and the SR Ca^{2+}-ATPase-1 (SERCA-1) is the predominant isoform in such SR preparations, as previously described [46].

2.3. Evaluation of Ca^{2+}-ATPase activity

Ca^{2+}-ATPase activity was measured spectrophotometrically at 22 °C using the coupled enzyme pyruvate kinase/lactate dehydrogenase assay, as described elsewhere [7,13,44,46,48,49], under the following conditions: 25 mM HEPES (pH 7.0), 100 mM KCl, 5 mM $MgCl_2$, 50 μM $CaCl_2$, 2.5 mM ATP, 0.42 mM phosphoenolpyruvate, 0.25 mM NADH, 18 IU lactate dehydrogenase and 7.5 IU pyruvate kinase, with or without Metf-V_{10}. The experiments were initiated by the addition of 10 μg/mL Ca^{2+}-ATPase, in the presence and absence of 4% (*w*/w) of the calcium ionophore A23187, and followed for 5 min, as described below. Briefly, freshly prepared Metf-V_{10} solutions were added to the medium immediately prior to SR Ca^{2+}-ATPase addition. The ATPase activity and the inhibition were measured taken into consideration the decrease of the OD per minute in the absence (100%) and in the presence of Metf-V_{10} solutions, as previously described [7,13,48]. After the addition of the enzymes to the medium, NADH was added followed by the vesicles containing Ca^{2+}-ATPase. Finally, after the addition of ATP, the absorbance was recorded during about 1 min (basal activity). After adding the ionophore, the subsequent decrease of the absorbance was measured during about 2 min (uncoupled ATPase activity). All experiments were performed at least in triplicate. The inhibitory power of the investigated Metf-V_{10} was evaluated, determining IC_{50} values meaning the POV concentration inducing 50% of Ca^{2+}-ATPase inhibition of the enzyme activity.

2.4. Cell culture and treatments

Human melanoma cell line UACC-62 (ATCC) and non-cancerous HEK293T cells (ATCC) were maintained in high glucose Dulbecco's Modified Eagle's Medium (DMEM) (Cytiva SH30243.LS), supplemented with 10% heat inactivated FBS (Corning Media Tech 35–079-CV) and antibiotics (penicillin (100 U/mL) and streptomycin (100 mg/mL) (A8943.0100, Panreac Applichem), in a humidified incubator at 37 °C (5% CO_2). Cells were cultured in cell culture dishes and flat bottom multiwell plates of crystal–grade polystyrene from SPL Life Sciences (10-cm dishes, 6-well and 96-well plates). Before splitting, cells were washed with phosphate buffer saline (PBS) and then added trypsin (Sigma-Aldrich, 59427C) to detach from the dishes, before being resuspended with complete DMEM.

Metformin (Cayman Chemical Company, 13118) and phenformin (Cayman Chemical Company, 14997) were prepared in PBS and DMSO, respectively. Calyculin A was from Santa-Cruz Biotechnology (sc-24000). Metf-V_{10} [40] was dissolved in 10% DMSO. Decavanadate (V_{10}) and vanadate (V_1) were prepared as described above. During treatments, DMSO was used as vehicle control. Pilot selected cellular experiments confirmed that DMSO at 0.1% was not toxic to cells neither influenced the results, when compared to cells without DMSO (not shown).

2.5. Cellular viability metabolic assay

Cells viability was determined using the 3-(4,5-dimethylthiazol-2-yl)-2,5-diphenyltetrazolium bromide (MTT) colorimetric assay, based on the ability of succinic dehydrogenase (SDH) of living cells to reduce the yellow salt MTT (Alfa Aesar, L11939, thiazolyl blue tetrazolium bromide 98%) to a purple-blue insoluble formazan precipitate [50]. The assay was performed in a 96-well plate, and normalized to control vehicle-treated cells, as a standard procedure. Briefly, 24 h after plating, the plating medium was removed and replaced by 100 μL of fresh DMEM along with the indicated respective treatments. After the designated time of treatment, DMEM was eliminated and 100 μL of MTT solution (0.5 mg/mL in DMEM) was added, and plates were incubated at 37 °C (5% CO_2) for additional 3 h. After that period, medium was aspirated and 100 μL of DMSO was added to each well to dissolve the crystal formed, and the amount of formazan formed was measured at 560 nm using a microplate reader (GLOMAX Multi Detection System, Promega). Three wells per condition were analyzed in at least three independent experiments. Absorbance at 750 nm was measured as internal negative control and was subtracted from the 560 nm absorbance values for all wells, as normalization (Norm). Cellular viability fold change to control was calculated as (Norm Abs560 sample – Norm Abs560 blank) / (Norm Abs560 control – Norm Abs560 blank). Blank correspond to wells without cells. Dose-response plots (log [drug (μM)] *vs* cell viability (%)) and non-linear regression were used to calculate IC_{50} values, using GraphPad Prism.

2.6. Cellular death trypan blue exclusion assay

The trypan blue exclusion test of cell viability was performed based on previously described procedures [51]. Briefly, UACC-62 cells were cultured in 6-well plates. After treatments, the media were fully collected from each plate to 15 mL conical tubes. Cells were additionally washed with PBS, which was collected to the previous tube. Trypsin was added to the plate, and after incubated for 5 min in a humidified incubator at 37 °C (5% CO_2), all cells were detached and were collected, once again, to the same conical tube. After this, cells were centrifuged at room temperature for 5 min at 250 x *g*. The supernatant was carefully discarded, and cells were resuspended in a determined volume of DMEM (from 50 to 200 μL, depending on the size of the obtained pellet). To prepare cells for counting, 10 μL of trypan blue (Amresco, K940, 0.4% aqueous solution) were mixed with 10 μL of the cell suspension, from which 10 μL were transferred to a hemocytometer (Neubauer chamber). Cells were manually counted separately at a brightfield microscope, where those unstained (white) were considered viable, and those blue-stained were considered dead cells.

2.7. Cell cycle analysis by flow cytometry

For cell cycle analysis, UACC-62 cells were plated in 10-cm dishes. After 24 h, cells were treated with either growth medium with 0.1% DMSO alone (control) or Met-V_{10} (10 μM), V_{10} (10 μM) and V_1 (100 μM). At 24 h following drugs treatments, cells were harvested by trypsinization and washed twice with PBS. Cells were resuspended in 50 μL cold PBS, fixed in 950 μL cold 70% ethanol and incubated at 4 °C for at least 30 min. Fixed cells were then centrifuged and washed twice with ice-cold PBS. After a last centrifugation, the supernatant was decanted, and the cells were resuspended and incubated in 650 μL PBS containing 20 μg/mL propidium iodide (PI) and 0.2 mg/mL RNase (Sigma-Aldrich, R6148). Flow cytometry was performed at the FACScalibur cell analyzer (BD Biosciences) to analyze DNA content, collecting fifty thousand PI positive gated events per sample. The cell cycle distribution data was obtained by applying the Watson Pragmatic model at the FlowJo software v7.6.1.

2.8. Protein extraction and Western blotting

For total protein extraction, UACC-62 cells were cultured in 10-cm dishes. For each condition and time-point, media were aspirated, cells were washed with cold PBS twice and were collected on ice with a scraper. After centrifugation, the pelleted cells were lysed in a home-made lysis buffer (20 mM Tris pH 7.5, 150 mM NaCl, 1% Triton X-100, 50 mM NaF, 1 mM EDTA, 1 mM ethylene glycol-bis(β-aminoethyl ether)-*N*,*N*,*N*′,*N*′-tetraacetic acid (EGTA), 2.5 mM sodium pyrophosphate, 1 mM b-glycerophosphate), supplemented with a protease inhibitor cocktail (Pierce, Thermoscientific, A32955) and calyculin A (10 nM, sc-24,000), by intermittent shaking for 20 min at 4 °C. Samples were centrifuged at 13800 x*g* for 20 min at 4 °C, and the supernatant corresponding to the protein extract was collected and frozen at −80 °C until use. Proteins in the extracts were quantified by the standard Bradford assay (J61522-K2 Alfa Aesar) [47].

For Western blot analysis, 50 μg of total protein was separated on 8% SDS-PAGE gel and transferred to a polyvinylidenedifluoride transfer membrane (PVDF) (10,600,021 Amersham Hybond 0.2 PVDF GE Healthcare Life Sciences) for 2 h at 75 V, using transfer buffer (60 mM Tris, 48.75 mM glycine, 20% methanol). Membranes were blocked by incubation in blocking buffer (Tris-buffered saline (TBS) containing 0.1% Tween (TBS-T) and 5% dried nonfat milk) for at least 1 h at room temperature, rinsed in TBS-T, and then blotted overnight at 4 °C with the indicated primary antibodies diluted in TBS-T and 5% BSA (Sigma-Aldrich) with 0.05% of sodium azide (Fisher Chemical S/2380/48). Blots were washed 4 times for 7 min with TBS-T and incubated for at least 1 h at room temperature with horseradish peroxidase-linked secondary antibodies (1:10000). After washing the membranes, blots were developed by freshly prepared enhanced chemiluminescence (ECL) detection solution (1.25 mM luminol, 0.198 mM p-Coumaric acid, 0.009% H_2O_2, 0.1 M Tris) and bands were visualized by chemiluminescence (ChemiDocXRS Imaging System, BioRad). Specific primary polyclonal antibodies for phosphorylated (P-) or total (t-) proteins detection were rabbit P-AKT (Ser473) (#4060), rabbit P-AKT (Thr308) (#4056), rabbit t-AKT (#9272), rabbit P-p44/42 MAPK (ERK1/2) (Thr 202/Tyr204) (#4370), rabbit P-AMPK (Thr172) (#2535), rabbit t-AMPK (#2532), rabbit P-p70 S6 Kinase (S6K) (Thr389) (#9234), and rabbit P-signal transducer and activator of transcription 3 (STAT3) (Tyr705) (#9145), purchased from Cell Signaling Technology (CST), and rabbit t-S6K (sc-230), rabbit t-ERK1/2 (sc-94), mouse t-STAT5 (sc-74,442) and rabbit glyceraldehyde 3-phosphate dehydrogenase (GAPDH) (sc-25,778), purchased from Santa Cruz Biotechnology (SCB). Mouse monoclonal anti-α-tubulin antibody (T9026) was from Sigma-Aldrich. Secondary antibodies were ECL Mouse IgG, horseradish peroxidase (HRP)-linked whole Ab (from sheep) (NA931) and ECL Rabbit IgG, HRP-linked whole Ab (from donkey) (NA934), both from GE Healthcare Life Sciences. When indicated, bands obtained from the western blots were quantified using the semi-quantitative software ImageJ/FIJI [52].

2.9. Statistical analysis

Data are expressed as mean ± SEM of at least three independent experiments, as indicated in figure legends. Statistical analysis was performed by using independent unpaired *t*-tests (with Welch's correction) or ANOVA, when more than two groups were being compared, as specified, using GraphPad Prism 8.4.0 software (GraphPad Software Inc., San Diego, CA, USA). A $p < 0.05$ was considered statistically significant.

3. Results

3.1. Inhibition of Ca^{2+}-ATPase by metformin-decavanadate (Metf-V_{10})

The antitumor activity of POMs is partially due to the inhibition of

specific enzymes such as alkaline phosphatases, kinases, ecto-nucleotidases, glucosidades as well as P-type ATPases, such as Na^+/K^+-ATPases and Ca^{2+}-ATPases [8]. Here, we investigated for the first time the effect of metformin-decavanadate (Metf-V_{10}) on the activity Ca^{2+}-ATPase from skeletal muscle, an established *in vitro* model previously used to evaluate polyoxometalates (POMs) and other metallocompounds [7,12,13,19,44,46,48,49]. We observed that Metf-V_{10} inhibits the Ca^{2+}-ATPase activity in a concentration dependent manner (Fig. 1A). The inhibitory capacity was evaluated using the IC_{50} values (compound concentration capable of inducing 50% inhibition of Ca^{2+}-ATPase enzyme activity). For Metf-V_{10}, an IC_{50} value of 87.4 μM was obtained (Fig. 1A). This value is about six times higher than the Ca^{2+}-ATPase IC_{50} values of inhibition that were previously determined for decavanadate (IC_{50} = 15 μM), under the same experimental conditions [48].

For others POTs and POVs, such as P_2W_{18} and PV_{14}, a mixed type inhibition was previously observed [7,13], while decavanadate (V_{10}) was previously characterized as a Ca^{2+}-ATPase non-competitive inhibitor [48]. To identify the type of inhibition of the Metf-V_{10} complex, concentrations near the IC_{50} values described above, were used. It was observed that Metf-V_{10} presented a mixed type inhibition (Fig. 1B). These observations suggest that Metf-V_{10} can interact with the Ca^{2+}-ATPase independent of the presence of a bound substrate. This indicates that there might be at least two distinct protein binding sites, where one of them is probably the ATP binding site.

3.2. Metformin-decavanadate (Metf-V_{10}) treatment leads to decreases of cellular viability in human melanoma UACC-62 cells

In order to explore a putative therapeutic potential of metformin-decavanadate (Metf-V_{10}) for the treatment of patients with melanoma, we investigated the effects of this compound in melanoma cells from human origin. To determine whether the complex Metf-V_{10} can inhibit the proliferation of melanoma cells, we investigated its effect in cell viability using the colorimetric metabolic assay MTT. Metf-V_{10} treatment (10 μM) for 48 h in human melanoma UACC-62 cells leads to decreases around 70% of cellular viability (Fig. 2A), which is equivalent to biguanides metformin (Metf) or phenformin (Phen) treatment, though at a lower concentration [50 mM Metf (Fig. 2B) or 1 mM Phen (Fig. 2C)]. When testing different concentrations and duration of treatment, we also found a significant dose-dependent decrease in cell viability, both after 48 h (Supp Fig. S1A) and 72 h (Supp Fig. S1B) of treatment with increasing concentrations of Metf-V_{10}. Increasing the time of treatment at the same doses, also led to an increased degree of reduction of the cellular viability (Supp Fig. S1A, S1B), where 5 μM Metf-V_{10} reduced 60% and over 80% viability after 48 or 72 h, respectively. As suggested previously [53], from these results we can endorse that Meft-V_{10} might be a more effective treatment than metformin in melanoma.

3.3. Comparable IC_{50} values for decavanadate (V_{10}) and metformin-decavanadate (Metf-V_{10}) in UACC-62 cells

To determine whether the effects observed in the inhibition of cellular viability were specific to the hybrid POM Metf-V_{10}, UACC-62 cells were treated with serial dilutions of either Metf-V_{10}, V_{10} or V_1. After a treatment of 48 h, we determined that the cell proliferation IC_{50} values for Metf-V_{10} (Fig. 3A), decavanadate (V_{10}) (Fig. 3B) and vanadate (V_1), (Fig. 3C), were 2.5 μM, 3.2 μM and 25.0 μM, respectively.

After 72 h of incubation with Metf-V_{10}, V_{10} and V_1, we observed a reduction in the percentage of viable cells of 87%, 85% and 86%, respectively (Supp Fig. S1B, S1C, S1D). Metf-V_{10} exposure at 50 μM for 3 h showed a 22% reduction on UACC-62 cells viability. Additionally, treatment with V_{10} (50 μM) or V_1 (500 μM) also reduced cell viability to 13% and 16%, respectively (Supp Fig. S2A, S2B, S2C). These comparable degrees of inhibition of cell viability by these different vanadium-based compounds, hampers the distinctiveness of the action of such molecules in an *in vivo* cellular system.

3.4. Metformin-decavanadate (Metf-V_{10}), decavanadate (V_{10}) and vanadate (V_1) induce cell cycle arrest in UACC-62 cells

To investigate whether the decreased cellular viability observed in UACC-62 cells, in response to Met-V_{10}, V_{10} or V_1 (Figs. 3B, C, S2B, S2C), was preferentially a response to cell death (cytotoxicity) or cell growth arrest (cytostasis), cellular death was evaluated by trypan blue exclusion assay, after a treatment of 24 h. As anticipated, a shorter period of incubation with Met-V_{10} (10 μM), V_{10} (10 μM) or V_1 (100 μM) led to a milder decrease in cellular viability (reduction of around 25% compared to control, evaluated as previously for 48 and 72 h of treatment), and also relatively similar between both compounds (Fig. 4A). By contrast, in non-malignant HEK293T cells, treatments with Met-V_{10}, V_{10} or V_1 for 24 h did not impair cell viability, and only after a treatment of 48 h a 15–20% reduction was observed (Supp Fig. S3A, S3B), suggesting that there might be a therapeutic window for these compounds.

Interestingly, the percentage of dead cells also showed a relatively mild difference between non-treated (vehicle control, 0.1% DMSO) *versus* Met-V_{10}, V_{10} or V_1-treated cells (varying from 7% to 16–22%, respectively) after a treatment of 24 h (Supp Fig. S4), which was comparable to the MTT results (Fig. 4A). By contrast, the total number of cells (alive *plus* dead) was reduced on average by 50% after either treatment compared to control cells (Fig. 4B). This suggested a greater impact on the cell cycle than in the activation of cell death mechanisms,

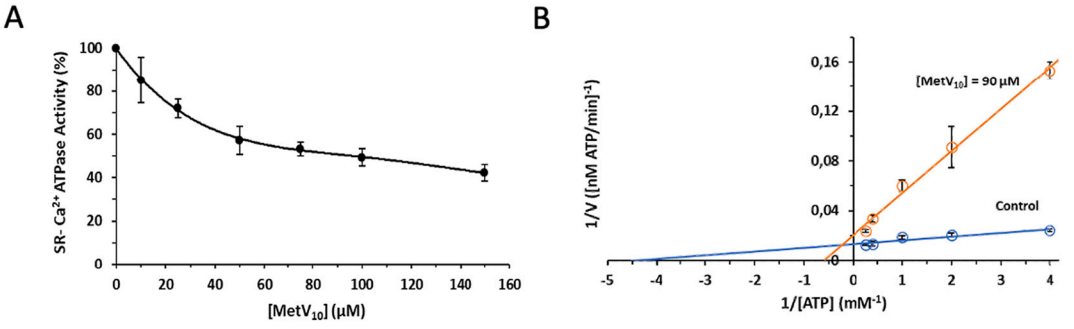

Fig. 1. Inhibition of Ca^{2+}-ATPase activity by metformin-decavanadate (Metf-V_{10}).
(A) Ca^{2+}-ATPase was measured spectrophotometrically at 340 nm and 25 °C, using the coupled enzyme pyruvate kinase/lactate dehydrogenase assay. The experiments were initiated after the addition of 10 μg/mL calcium ATPase. Equation used for the determination of the metformin-decavanadate ($MetV_{10}$) IC_{50} value: y = 3E-07 × ^{4}–0.0001 × ^{3} + 0.0209 × ^{2}–1.5958× + 99.816. An IC_{50} value of 87.4 μM was obtained for Metf-V_{10}. (B) Lineweaver-Burk plots of Ca^{2+}-ATPase activity in the absence (blue) and in the presence (red) of 50 μM Metf-V_{10}. The plots were used for determining the type of enzyme inhibition. Km values of 0.22 and 1.64 (mM) and Vmax values of 74.63 and 48.54 (nM ATP/min), were obtained in the absence and in the presence of $MetfV_{10}$, (90 μM) respectively, pointing out to a mixed type of inhibition. (A, B) Data are plotted as means ± SD. The results shown are the average of triplicate experiments carried out in distinct protein preparations.

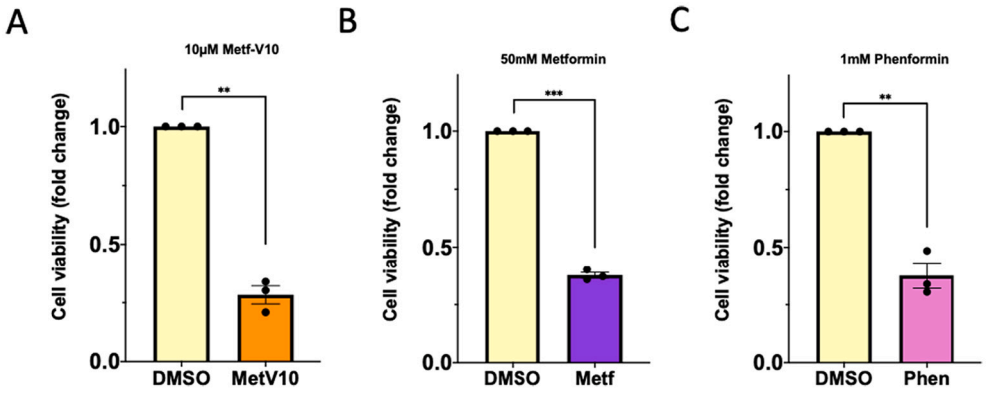

Fig. 2. Inhibition of cellular viability in response to 48 h treatments with Metf-V_{10} *vs* biguanides.
Cells viability was measured through MTT colorimetric assay, represented as fold change to vehicle-treated control cells (DMSO). For each experiment, 3000 cells/well were plated in a 96-well plate and treated the following day with 10 μM Metf-V_{10} (A), 50 mM metformin (Meft) (B) or 1 mM phenformin (Phen) (C), diluted in complete DMEM (100 μL/well). After 48 h, cell media were removed and replaced with 100 μL fresh medium containing MTT solution (0.5 mg/mL). After 3 h, media were eliminated and 100 μL of DMSO were added to dissolve the formazan crystals formed in metabolically active cells, prior to the measurement of absorbance. Statistical significance was determined by unpaired *t*-test, with ** $p < 0.01$, *** $p < 0.001$, as indicated in each graph. The mean ± SEM from three independent experiments in triplicate is shown.

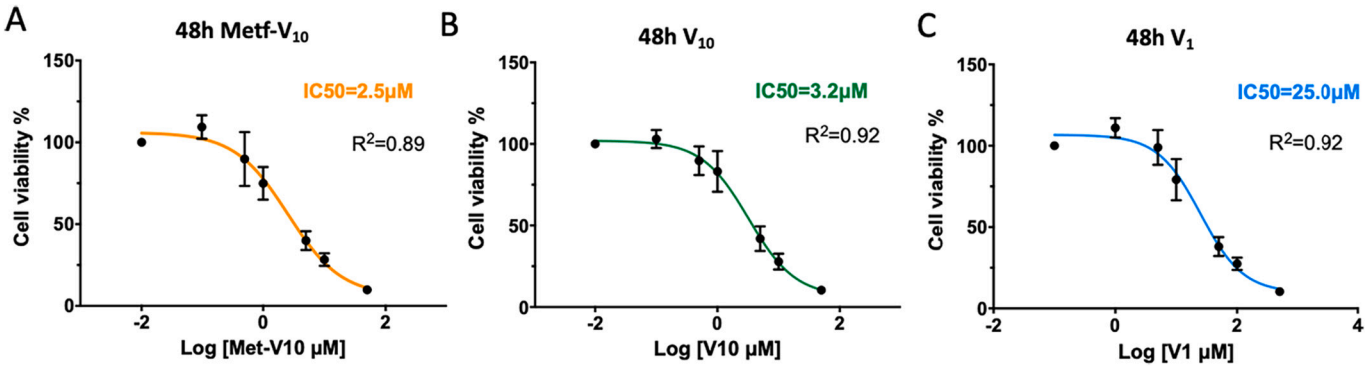

Fig. 3. Dose-response (IC_{50} determination) to vanadium compounds.
UACC-62 cells were treated with serial dilutions of Metf-V_{10} (A) or V_{10} (B) [0.1; 0.5; 1; 5; 10; 50 μM], or V_1 (C) [1; 5; 10; 50; 100; 500 μM], for 48 h. Cell viability % was determined to generate dose-response plots (obtained by MTT assay, as for Fig. 2). The mean ± SEM from three independent experiments in triplicate is shown.

similarly by both Met-V_{10}, V_{10} and V_1, though with the latest cells were incubated at a 10-times higher concentration (10 μM of Met-V_{10} or V_{10} *vs* 100 μM of V_1). To validate such hypothesis, we performed cell cycle analysis using flow cytometry. We observed a statistically significant decrease in the distribution of the cells at G1, and an increase in the G2/M phase, indicating a cell cycle arrest after all treatments compared to vehicle control (Fig. 4C, D).

3.5. *Increased MAPK/ERK and PI3K/AKT signaling pathways after POVs treatment in UACC-62 cells*

In order to examine whether the tested POVs modulate key pathways in cancer development and progression, we monitored the MAPK/ERK and PI3K/AKT signaling pathways in UACC-62 cells upon compound exposure at different time-points. First, we observed that both V_{10} and Meft-V_{10} were able to increase the levels of phosphorylation of the serine/threonine kinase AKT and the extracellular signal-regulated kinase (ERK), and that this effect, which was time-dependent, was independent of the complex used (Figs. 5A, B, S5A, S5B, S5C, S5D). Indeed, early after 3 h, increased P-AKT (Ser473) and P-ERK1/2 levels were observed in both Metf-V_{10} and V_{10} treated cells compared to control vehicle-treated cells, which was increasingly sustained until 24 h (Fig. 5A, B). Increases in P-AKT (Ser473) were also clearly dose-dependent (Fig. 5A, B), achieving on average a 7-fold increase at the maximal duration and concentration tested, independent of the vanadate complex used (Fig. S5E). Highly hyperactivated ERK and AKT pathways may induce cell cycle arrest [54,55], which fits with the previous results (Fig. 4C, D).

Vanadate (V_1) is a protein tyrosine phosphatase (PTP) enzyme inhibitor [56], which may lead to the impairment of the the phosphotyrosine signaling. To better understand whether the observed increased phosphorylation of ERK and AKT was due to intracellular phosphatases inhibition, UACC-62 cells were also treated with the phosphatase inhibitor calyculin A [57]. Cells were treated with calyculin A for 24 h followed by protein extraction. However, while 24 h treatments with all three vanadium-based compounds (Meft-V_{10}, V_{10} and V_1) led to increased levels of phosphorylated AKT and ERK, treatment with calyculin A did not result in higher phosphorylation (Fig. 5C). Importantly, increased AKT phosphorylation was not only detected at the Ser473 residue, but also at Thr308, which occur by different kinases [58,59], meaning this could still indicate a global increased protein phosphorylation based on the POVs phosphatases inhibition. To further explore this hypothesis, we also evaluated the phosphorylation status of additional proteins, involved in different important cancer signaling pathways, such as AMP-activated protein kinase (AMPK), p70 ribosomal S6 kinase (S6K) and signal transducer and activator of transcription 3 (STAT3). Nevertheless, while STAT3 phosphorylation at the Tyr705 residue was also induced, we were not able to detect differences in S6K phosphorylation (Thr389), nor in AMPK phosphorylation (Thr172), in response to Meft-V_{10}, V_{10}, V_1 nor calyculin A treatments (Fig. 5C). We additionally verified that, while 10 μM of V_1 did not affect the levels of P-ERK1/2 or P-AKT, V_1 at the 100 μM concentration led to comparable effects with Meft-V_{10} or V_{10} at the 10 μM dose (Fig. 5C). These results suggest that specific pathways are being modulated by such POVs, and

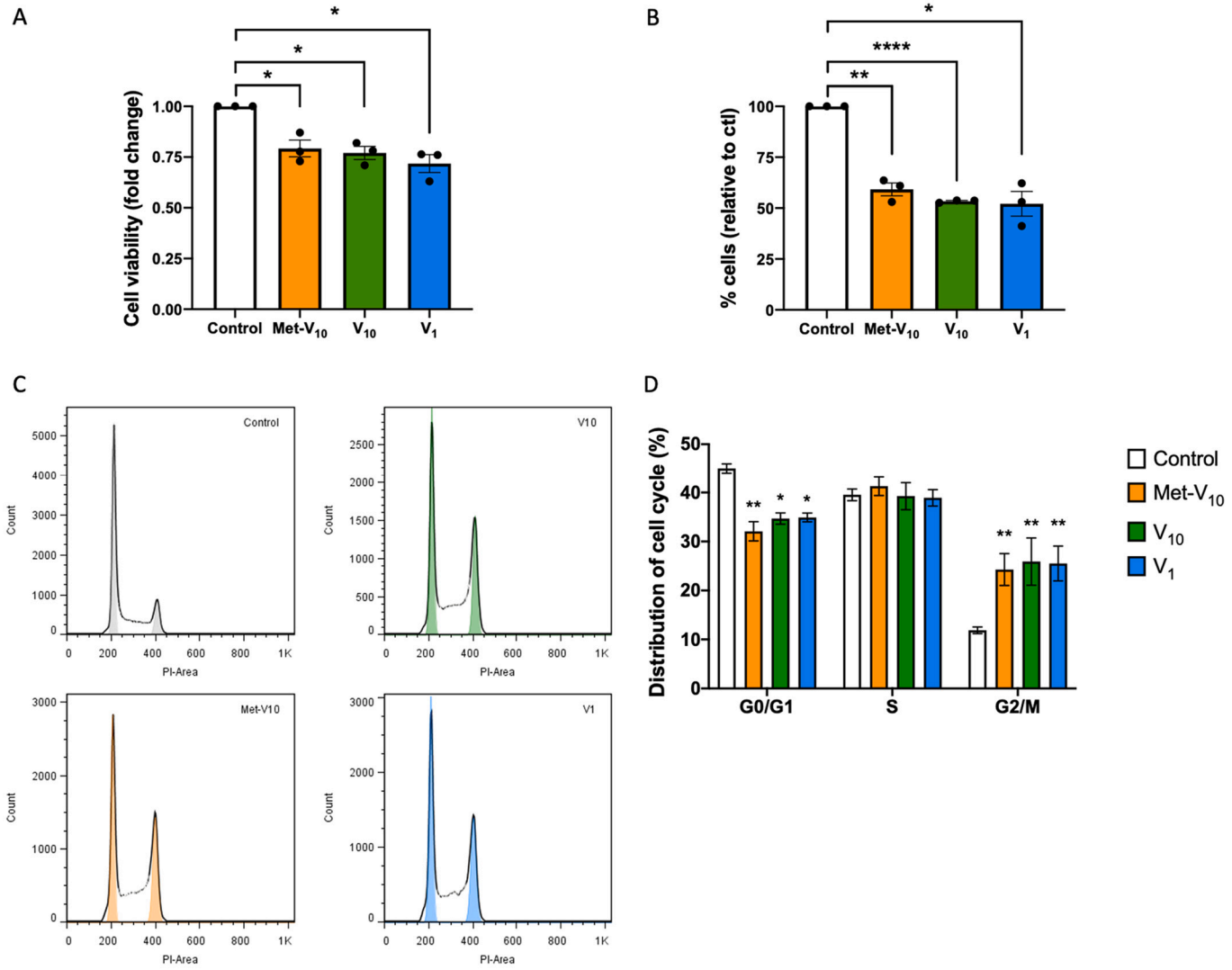

Fig. 4. Inhibition of cellular proliferation in response to 24 h treatments with metformin-decavanadate (Metf-V_{10}), decavanadate (V_{10}) or vanadate (V_1). (A) Cells viability was evaluated by MTT assay after treatment for 24 h with either Met-V_{10} (10 μM), V_{10} (10 μM) or V_1 (100 μM), and is represented as fold change to control (as previously described for Fig. 2). (B) Cells numbers are shown as % to control wells without treatments (vehicle control, ctl), considering both live and dead cells. For each experiment of cell counting, 100,000 cells/well were plated in a 6-well plate. The following day medium was removed and replaced with fresh medium with Met-V_{10}, V_{10} or V_1 at the indicated doses for 24 h before collection. (C) Flow cytometry was used to determine the cell cycle distribution of UACC-62 cells. The area under the curves for G1 and G2/M, used for the cell cycle analysis, are highlighted in color. A representative experiment is shown. (D) Analysis of the cell cycle distribution by employing a mathematical model (Watson) using FlowJo software. For each of such experiments, 1,000,000 cells/10-cm dish were plated. The following day medium was removed and replaced with fresh medium with Met-V_{10}, V_{10} or V_1 at the indicated doses for 24 h before collection. Statistical significance was determined by independent unpaired *t*-test, with * $p < 0.05$, ** $p < 0.01$, compared to control, as indicated in each graph. The mean ± SEM from three independent experiments is shown for each assay.

that the observed effects are not due to overall protein phosphorylation, though the exact mechanisms remain unknown.

4. Discussion

Polyoxovanadates (POVs) have become of great interest in biomedical studies, since they are known to have anticancer, antibacterial and antiviral activities by targeting many key cellular proteins [8,60,61]. Decavanadate (V_{10}) is probably the most studied POV [14,62]. In cancer research, it was previously described that V_{10} reduced the viability of both human hepatocellular (SSMC-7721) and ovarian (SK-OV-3) carcinoma cell lines after 72 h of treatment [63]. While also evaluated in different breast and lung cancer representative cell lines [87–89], among other types of cancer (Table S1), V_{10} had never been tested in melanoma cells. V_{10} was also described as a potent P-type ATPase inhibitor [13,48], which might be related with its anti-tumor activity. Both *ex vivo* Na^+/K^+-ATPase and *in vitro* Ca^{2+}-ATPase assays, previously showed greater degree of inhibition at the same concentration (10 μM) and a lower IC_{50} for V_{10} when compared to V_1, namely 66% *vs* 33%, and 15 μM *vs* 50 μM, respectively [13,48]. A compound containing the metforminium cation and the decavanadate anion (Metf-V_{10}) was previously synthesized [38]. Herein, we evaluated for the first time the effect of Metf-V_{10} and found that it is around 6 times less potent than V_{10} at inhibiting the ion pump Ca^{2+}-ATPase (87 μM *vs* 15 μM) (Table 1).

The IC_{50} value obtained for Metf-V_{10} was also over 2-times higher than what was verified for decaniobate $[Nb_{10}O_{28}]^{6-}$ (IC_{50} = 35 μM) [48]. Similar values of P-type ATPase inhibition were previously determined for some other POVs and polyoxotungstates (POTs), such as MnV_{11} (IC_{50} = 58 μM) and TeW_6 (IC_{50} = 200 μM) [7,44]. By contrast, IC_{50} values below 1 μM were previously determined for POTs, such as P_2W_{18} (0.6 μM), Se_2W_{29} (IC_{50} = 0.3 μM), and also for PV_{14} (IC_{50} = 1 μM) [7,13] (Table 1). Note that the SERCA and plasma-membrane calcium

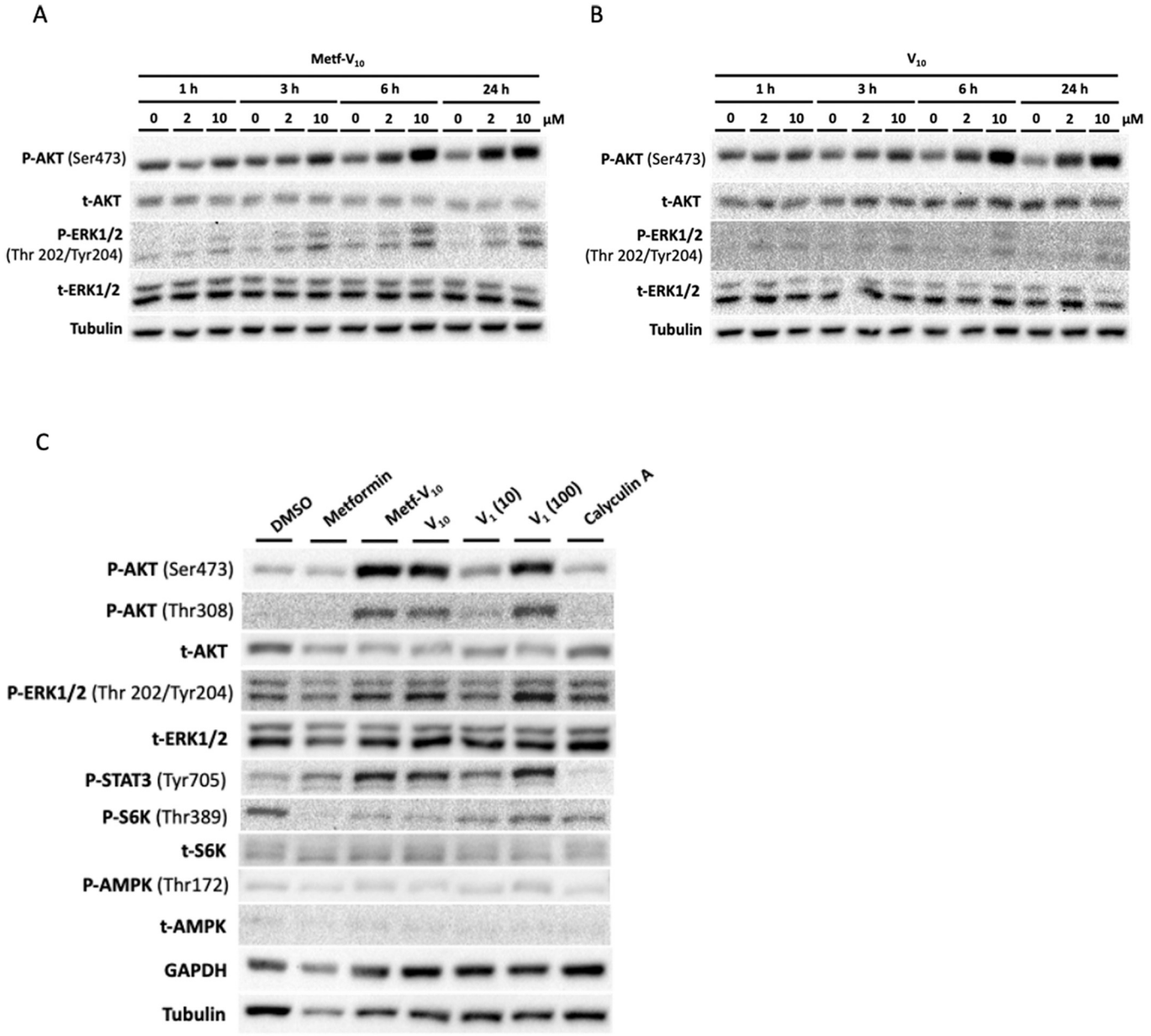

Fig. 5. AKT and ERK signaling pathways activation after vanadate complexes treatment.
Time-course and dose-dependent effect of Metf-V_{10} (A) and V_{10} (B) in the levels of phosphorylated AKT (Ser473) and ERK1/2 (Thr 202/Tyr204), normalized to the total proteins. (C) Effect of metformin (Metf), Metf-V_{10}, V_{10}, V_1, and calyculin A, after a 24 h incubation, in the levels of phosphorylated AKT (Ser473, Thr308), ERK1/2 (Thr 202/Tyr204), STAT3 (Tyr705), AMPK (Thr172) and S6K (Thr389). DMSO (0.1%) was used as vehicle control. Calyculin A is an inhibitor of the protein phosphatases type 1 (PP1) and type 2A (PP2A), which dephosphorylate serine and threonine residues [57]. For each experiment, 1,000,000 cells were plated in a 10-cm dish and treated the following day with the indicated treatments. After the indicated time-point, cell pellet was collected and the proteins extracted, quantified and prepared for electrophoresis and blotting with the indicated primary antibodies. Tubulin (A,B,C) and GAPDH (C) were used as loading controls.

Table 1
P-type ATPases inhibition values.

Compound	Ca^{2+}-ATPase IC_{50} (μM)	References
Se_2W_{29}	0.3	[7]
P_2W_{18}	0.6	[7]
TeW_6	200	[7]
PV_{14}	1	[13]
MnV_{11}	58	[44]
Nb_{10}	35	[48]
V_1	50	[48]
V_{10}	15	[48]
Metf-V_{10}	87	This study

pumps (PMCA) P-type ATPases are well known to be inhibited by metal (such as V, W and Au) complexes and compounds, and some of them showed values comparable with clinical used drugs [7,12,13,18,49]. Here, we verified that Metf-V_{10} complex is not a strong inhibitor of the calcium pump (IC_{50} = 87 μM), and that it presents a mixed type inhibition. This is in contrast with previous results for both V_{10} and Nb_{10}, which were characterized as Ca^{2+}-ATPase non-competitive inhibitors [48]. However, virtually nothing is known, to the majority of POMs species, about the protein conformations favourable for interaction and binding sites with some exception investigating V_{10} and Nb_{10} with Ca^{2+}-ATPase [48]. In these studies, it was referred that conversely to V_1, which only binds to the E2 conformation of the Ca^{2+}-ATPase, V_{10} binds strongly to all conformations either E1 or E2, being or not

phosphorylated [48,64]. Contrariwise, for some drugs such as thapsigargin and cyclopiazonic acid, the mechanisms of action and ATPases binding sites were clearly established [65]. It is very important to note that for the determination of the IC_{50} values and the type of inhibition described above, the Metf-V_{10} compound was added to the medium immediately before the beginning of the reaction being the rate measure within the next 2–3 min. The kinetics of the decomposition reaction of V_{10} as well as of Metf-V_{10} was previously determined by UV/Vis and ^{51}V NMR spectroscopy [45,66]. It was described that after addition of V_{10} and/or Metf-V_{10} in the medium, intact V_{10} species with amounts of vanadate oligomers were detected [21,45,66]. Thus, considering the absence of incubation and the short period used for measuring the ATPase activity, it is possible to suggest that the inhibitory effects and the type of inhibition described are due to Metf-V_{10} specifically.

When treating the UACC-62 human melanoma cells in culture, we found a very similar degree of inhibition of cellular viability, independent of either treating the cells with Metf-V_{10} or V_{10}, or even with a 10-fold higher concentration of V_1. By contrast, in HepG2 hepatoma cells, although V_{10} and Metf-V_{10} also inhibited cellular viability, a 3-fold difference in the calculated IC_{50} (9 μM *vs* 29 μM, respectively) was achieved for 24 h treatment [45]. This disparity could be a reflection of intrinsic differences among cell lines and cellular pathways involved. However, there are still few studies reporting the effects of POMs in melanoma cell lines, namely polyoxomolybdates [67,68].

Vanadium speciation is complicated under physiological conditions, strongly depending on the concentration of vanadium, the pH of the solution, and ionic strength [69,70]. Eventually, decavanadate anion and the metformin-decavanadate compound (Metf-V_{10}) once inside its target cells, may both undergo decomposition, complexation with other compounds, reduced by oxidants and/or may release their bound molecules [71]. The kinetics of the decomposition reaction of Metf-V_{10} in DMEM medium was recently determined by ^{51}V NMR spectroscopy [45]. After dissolving Metf-V_{10} in the cell culture medium, intact V_{10} species were detected after 24 h, among other vanadium species such as orthovanadate (V_1) and metavanadate species V_2, V_4 and V_5, that are formed over time [45]. It was clear from these NMR spectra at this timepoint that V_1 signal is broadened, suggesting formation of a vanadate complex with other compounds present in the medium. The decomposition of Metf-V_{10} compound shows first-order dependence *versus* time. The calculated lifetime for Metf-V_{10} was found to be about 9 h and 11 h for 0.5 mM and 1 mM concentrations [45]. These results are in line with the half-life time for the decomposition of decameric species found by Ramos et al. [66]. However, in these studies, it was demonstrated that the presence of proteins, such as actin and Ca^{2+}-ATPase, impede the decomposition of V_{10}, whereas no changes were observed for the muscular protein myosin and for lipid structures such as liposomes [66]. In fact, it was observed that the half-life time of V_{10} decomposition increases from 5 to 15 and to 27 h, in the presence of Ca^{2+}-ATPase and G-actin, respectively [66]. Note that the isopolyoxovanadate decavanadate (V_{10}) is perhaps the most studied regarding its stability at biological conditions [15,62,64,66,72–74]. Thus, even considering that in the cellular medium the studied POVs are not completely stable at the experimental medium, it can be assumed that the presence of specific cellular targets would prevent V_{10} and Metf-V_{10} decomposition and favoring the induction of a specific biological effect, namely ATPase activity and cellular proliferation inhibition.

Cellular signaling modulation is very relevant in cancer development and progression, and changes may occur early in time after treatments. For instance, the MAPK/ERK and PI3K/AKT pathways are important signaling axes aiding cancer cells proliferation and survival [75]. Activated extracellular regulated kinases (ERK) have been classically described as important positive regulators of cell cycle and tumor progression [76]. Intricately, vanadium compounds can activate MAPK/ERK signaling pathway and still cause tumor suppression, due to the induction of an abnormal mitogenic signaling. Previous studies showed that the vanadium compounds sodium metavanadate ($NaVO_3$) and bis (acetylacetonato)-oxovanadium(iv) ($VO(acac)_2$), exhibited anti-proliferative effect through inducing G2/M cell cycle arrest, in the absence of induced apoptosis, in human pancreatic cancer AsPC-1 cells [77]. Such as in our study, the authors also found a sustained activation of PI3K/AKT and MAPK/ERK signaling pathways, which was both dose- and time-dependent, and suggested that the observed cell cycle arrest was a response for ERK, and not AKT, hyperactivation [77]. Consistently, both AKT and ERK signaling pathways were also highly activated in the human hepatoma HepG2 cells in response to $VO(acac)_2$ treatment, in which the latest was also associated with cell cycle progression blockage in G1/S phases [78]. Furthermore, treatment of the rat osteosarcoma UMR106 cells with the complex bis(aqua) oxodiacetatooxovanadium(IV) (VO(oda)), an organic derivative of vanadyl(IV) cation with oxodiacetate, led not only to decreased cellular proliferation [79], as stimulated ERK phosphorylation in a dose dependent manner [80]. These data are in agreement with our results showing reduced cellular viability and proliferation, cell cycle arrest, and both ERK and AKT signaling pathways hyperactivation in response to treatments with Metf-V_{10}, V_{10} or V_1. The inhibition of key protein tyrosine phosphatases (PTPs) might be among the possible antitumor mechanisms for the POVs and other vanadium-based complexes [81], which could lead to the induction of phosphorylation of tyrosine residues, and consequently the activation of these signaling pathways. Nevertheless, our data show that treatments with Metf-V_{10}, V_{10} and V_1 do not induce a global protein hyperphosphorylation. Serendipitously, we found evidence for the first time that Metf-V_{10}, V_{10} and V_1 led to the activation of the transcription factor STAT3, evidenced by its increased phosphorylation at Tyr705, in UACC-62 melanoma cells. This would allow STAT3 nuclear localization and eventually promoting tumor cell survival [82], which was not observed. The impact of such POVs on other STAT3 phospho-residues is also still to be further explored.

Early studies showed that the fast and transient ERK activation was induced after only 5 min of increasing concentrations (up to 1 mM) of vanadate (V_1) in CHO cells [83]. By contrast, however, it was recently described that in A375 human melanoma cells, treatment with 20 μM of the inorganic anion vanadate for 24 h, led to a decrease in P-ERK [27]. In this work, the authors justified the differences observed to the fact that A375 cells contain the prevalent V600E BRAF mutation [27], in contrast to other cancer (non-melanoma) cells, considering that the MAPK pathway would be constitutively hyperactivated [84]. Nevertheless, we have used UACC-62 human melanoma cells, which also harbor the V600E BRAF mutation, and our results showed a clear increase in P-ERK upon treatment with 100 μM. These results argue that the cellular response to these compounds is independent on the BRAF mutation status.

It is important to note that POMs-mediated impairments in cellular proliferation might not be fully tumor-cell-selective. In fact, we found a non-neglected effect of both Metf-V_{10}, V_{10} and V_1 in the non-cancer HEK293T cells after 48 h of treatment, though lower than observed in UACC-62 cancer cells for the same period of time (up to 20% *vs.* around 75% reduction in viability, in HEK293T compared to UACC-62, respectively). Accordingly, a 3–4 fold increase in the calculated IC_{50} value for a treatment of 24 h was also previously observed when comparing HEK293T cells with HepG2 cells for either Metf-V_{10} or V_{10} [45] (Table S1). In addition, incubation of cardiomyocytes with either 10 μM metavanadate (which contains monomeric vanadate, di-, tetra-, and pentavanadate) or 1 μM decavanadate (*i.e.*, 10 μM total vanadium), for the same period of time, induced necrotic cell death [72]. Others have also shown that while vanadium compounds inhibited normal L02 cell proliferation, an immortalized hepatic cell line, it was only at greater doses than those needed for HepG2 cancer cells [85] (Table S1). Nevertheless, other vanadium-based compound, for instance vanadyl (IV) sulfate ($VOSO_4$), was previously shown to inhibit the proliferation and to induce apoptosis in human normal keratinocytes (HaCaT) [86]. For these reasons, it will be important to better determine the putative therapeutic window for these compounds to limit toxicity in normal

tissues.

The observed inhibitory effect in UACC-62 cells' proliferation of the tested vanadium compounds, suggests that these metallodrug complexes may be considered a potential treatment in melanoma. The hybrid POM metformin-decavanadate (Metf-V_{10}) showed an antiproliferative action at much lower concentrations, compared to metformin alone, in UACC-62 melanoma cells. It had been previously suggested that V_{10} and V_1 could act through different pathways [48], and that Metf-V_{10} had increased stability along with a potential lower intracellular biotransformation [53]. In the present study, the cellular effects of V_{10} and Metf-V_{10} were mainly considered undistinguishable. This might be partially due to the cellular experimental conditions, and so modifications of the potential metallodrugs delivery to the cells in culture would allow to further pursue and discriminate the mechanisms and the steps of the action involved for such hybrid POMs.

Author contributions

All authors listed have made a substantial, direct and intellectual contribution to the work, and approved it for publication.

Funding

This work was funded by the Spanish Ministry of Science, Innovation and Universities through grant RTI2018-094629-B-I00 to WL, and Fundação para a Ciência e a Tecnologia (FCT) (PTDC/MED-ONC/4167/2020 "ENDURING") to BIF.

Declaration of Competing Interest

The authors declare that the research was conducted in the absence of any commercial or financial relationships that could be construed as a potential conflict of interest. WL is cofounders of Refoxy Pharmaceuticals GmbH, Berlin. W.L. is required by his institution to state so in his publications. The other authors declare no conflict of interest.

Data availability

Data will be made available on request.

Acknowledgments

The authors acknowledge the Flow Cytometry Unit at Algarve Biomedical Center Research Institute (ABC-RI) for providing scientific and technical support during flow cytometry experiments, and specifically acknowledge the core technician Maurícia Vinhas for the full support during the assays and analyses. This study received Portuguese national funds from FCT - Foundation for Science and Technology through projects UIDB/04326/2020, UIDB/04326/2020 and LA/P/0101/2020.

Appendix A. Supplementary data

Supplementary data to this article can be found online at https://doi.org/10.1016/j.jinorgbio.2022.111915.

References

[1] E.L.M. Ochoa, Lithium as a neuroprotective agent for bipolar disorder: an overview, Cell. Mol. Neurobiol. 42 (1) (2022) 85–97.
[2] R. Bertinat, F. Westermeier, R. Gatica, F. Nualart, Sodium tungstate: is it a safe option for a chronic disease setting, such as diabetes? J. Cell. Physiol. 234 (1) (2018) 51–60.
[3] M.J.S.A. Silva, P.M.P. Gois, G. Gasser, Unveiling the potential of transition metal complexes for medicine: translational in situ activation of metal-based drugs from bench to in vivo applications, Chembiochem. 22 (10) (2021) 1740–1742.
[4] A. Ścibior, Ł. Pietrzyk, Z. Plewa, A. Skiba, Vanadium: risks and possible benefits in the light of a comprehensive overview of its pharmacotoxicological mechanisms and multi-applications with a summary of further research trends, J. Trace Elem. Med. Biol. 61 (2020) 126508. Sep.
[5] C. Yeo, K. Ooi, E. Tiekink, Gold-based medicine: a paradigm shift in anti-Cancer therapy? Molecules. 23 (6) (2018) 1410. Jun 11.
[6] C. Pimpão, I.V. da Silva, A.F. Mósca, J.O. Pinho, M.M. Gaspar, N.I. Gumerova, et al., The Aquaporin-3-inhibiting potential of Polyoxotungstates, Int. J. Mol. Sci. 21 (7) (2020) 2467.
[7] N. Gumerova, L. Krivosudský, G. Fraqueza, J. Breibeck, E. Al-Sayed, E. Tanuhadi, et al., The P-type ATPase inhibiting potential of polyoxotungstates, Metallomics. 10 (2) (2018) 287–295.
[8] A. Bijelic, M. Aureliano, A. Rompel, Polyoxometalates as potential next-generation Metallodrugs in the combat against Cancer, Angew. Chem. Int. Ed. Eng. 58 (10) (2019) 2980–2999.
[9] S.M. Corsello, R.T. Nagari, R.D. Spangler, J. Rossen, M. Kocak, J.G. Bryan, et al., Discovering the anticancer potential of non-oncology drugs by systematic viability profiling, Nat. Can. 1 (2) (2020) 235–248.
[10] Z. Hosseinzadeh, S. Hauser, Y. Singh, L. Pelzl, S. Schuster, Y. Sharma, et al., Decreased Na+/K+ ATPase expression and depolarized cell membrane in neurons differentiated from chorea-Acanthocytosis patients, Sci. Rep. 10 (1) (2020) 8391.
[11] M. Vosahlikova, L. Roubalova, K. Cechova, J. Kaufman, S. Musil, I. Miksik, et al., Na+/K+-ATPase and lipid peroxidation in forebrain cortex and hippocampus of sleep-deprived rats treated with therapeutic lithium concentration for different periods of time, Prog. Neuro-Psychopharmacol. Biol. Psychiatry 102 (2020), 109953.
[12] C. Fonseca, G. Fraqueza, S.A.C. Carabineiro, M. Aureliano, The Ca2+-ATPase inhibition potential of gold(I, III) compounds, Inorganics. 8 (9) (2020) 49.
[13] G. Fraqueza, J. Fuentes, L. Krivosudský, S. Dutta, S.S. Mal, A. Roller, et al., Inhibition of Na+/K+- and Ca2+-ATPase activities by phosphotetradecavanadate, J. Inorg. Biochem. 197 (2019), 110700.
[14] M. Aureliano, N.I. Gumerova, G. Sciortino, E. Garribba, A. Rompel, D.C. Crans, Polyoxovanadates with emerging biomedical activities, Coord. Chem. Rev. 447 (2021), 214143.
[15] M. Aureliano, N.I. Gumerova, G. Sciortino, E. Garribba, C.C. McLauchlan, A. Rompel, et al., Polyoxidovanadates' interactions with proteins: an overview, Coord. Chem. Rev. 454 (2022), 214344.
[16] G. Guedes, S. Wang, H.A. Santos, F.L. Sousa, Polyoxometalate composites in Cancer therapy and diagnostics, Eur. J. Inorg. Chem. 2020 (22) (2020) 2121–2132.
[17] M. Aureliano, The future is bright for Polyoxometalates, BioChem. 2 (1) (2022) 8–26.
[18] M. Aureliano, Decavanadate: a journey in a search of a role, Dalton Trans. 42 (2009) 9093.
[19] M. Aureliano, G. Fraqueza, C.A. Ohlin, Ion pumps as biological targets for decavanadate, Dalton Trans. 42 (33) (2013) 11770.
[20] D.C. Crans, J.J. Smee, E. Gaidamauskas, L. Yang, The chemistry and biochemistry of vanadium and the biological activities exerted by vanadium compounds, Chem. Rev. 104 (2) (2004) 849–902.
[21] M. Aureliano, D.C. Crans, Decavanadate (V10O286-) and oxovanadates: oxometalates with many biological activities, J. Inorg. Biochem. 103 (4) (2009) 536–546.
[22] G. Sciortino, M. Aureliano, E. Garribba, Rationalizing the Decavanadate(V) and Oxidovanadium(IV) binding to G-actin and the competition with Decaniobate(V) and ATP, Inorg. Chem. 60 (1) (2021) 334–344.
[23] G. Leonardi, L. Falzone, R. Salemi, A. Zanghì, D. Spandidos, J. Mccubrey, et al., Cutaneous melanoma: from pathogenesis to therapy (review), Int. J. Oncol. 52 (4) (2018) 1071–1080.
[24] M. Furue, T. Ito, N. Wada, M. Wada, T. Kadono, H. Uchi, Melanoma and immune checkpoint inhibitors, Curr. Oncol. Rep. 20 (3) (2018) 29.
[25] J.J. Luke, K.T. Flaherty, A. Ribas, G.V. Long, Targeted agents and immunotherapies: optimizing outcomes in melanoma, Nat. Rev. Clin. Oncol. 14 (8) (2017) 463–482.
[26] S. Das, A. Roy, A.K. Barui, M.M.A. Alabbasi, M. Kuncha, R. Sistla, et al., Anti-angiogenic vanadium pentoxide nanoparticles for the treatment of melanoma and their in vivo toxicity study, Nanoscale. 12 (14) (2020) 7604–7621.
[27] M. Pisano, C. Arru, M. Serra, G. Galleri, D. Sanna, E. Garribba, et al., Antiproliferative activity of vanadium compounds: effects on the major malignant melanoma molecular pathways, Metallomics. 11 (10) (2019) 1687–1699.
[28] C.L.A. Farias, G.R. Martinez, S.M.S.C. Cadena, A.L.R. Mercê, C.L. de Oliveira Petkowicz, G.R. Noleto, Cytotoxicity of xyloglucan from *Copaifera langsdorffii* and its complex with oxovanadium (IV/V) on B16F10 cells, Int. J. Biol. Macromol. 121 (2019) 1019–1028.
[29] C. Rozzo, D. Sanna, E. Garribba, M. Serra, A. Cantara, G. Palmieri, et al., Antitumoral effect of vanadium compounds in malignant melanoma cell lines, J. Inorg. Biochem. 174 (2017) 14–24.
[30] M. Strianese, A. Basile, A. Mazzone, S. Morello, M.C. Turco, C. Pellecchia, Therapeutic potential of a pyridoxal-based vanadium(IV) complex showing selective cytotoxicity for cancer versus healthy cells, J. Cell. Physiol. 228 (11) (2013) 2202–2209.
[31] C. Amante, A.L. De Sousa-Coelho, M. Aureliano, Vanadium and melanoma: a systematic review, Metals (Basel). 11 (5) (2021) 828.
[32] T.-T. Liu, Y.-J. Liu, Q. Wang, X.-G. Yang, K. Wang, Reactive-oxygen-species-mediated Cdc25C degradation results in differential antiproliferative activities of vanadate, tungstate, and molybdate in the PC-3 human prostate cancer cell line, J. Biol. Inorg. Chem. 17 (2) (2012) 311–320.
[33] Q. Yu, W. Jiang, D. Li, M. Gu, K. Liu, L. Dong, et al., Sodium orthovanadate inhibits growth and triggers apoptosis of human anaplastic thyroid carcinoma cells in vitro and in vivo, Oncol. Lett. 17 (5) (2019) 4255–4262.

[34] A.P. Gonçalves, A. Videira, P. Soares, V. Máximo, Orthovanadate-induced cell death in RET/PTC1-harboring cancer cells involves the activation of caspases and altered signaling through PI3K/Akt/mTOR, Life Sci. 89 (11–12) (2011) 371–377.
[35] J. Yang, Z. Zhang, S. Jiang, M. Zhang, J. Lu, L. Huang, et al., Vanadate-induced antiproliferative and apoptotic response in esophageal squamous carcinoma cell line EC109, J. Toxicol. Environ. Health A 79 (19) (2016) 864–868.
[36] A.A. Khalil, M.J. Jameson, Sodium Orthovanadate inhibits proliferation and triggers apoptosis in Oral squamous cell carcinoma in vitro, Biochemistry (Mosc) 82 (2) (2017) 149–155.
[37] T.M. Ashton, W.G. McKenna, L.A. Kunz-Schughart, G.S. Higgins, Oxidative phosphorylation as an emerging target in cancer therapy, Clin. Cancer Res. 24 (11) (2018) 2482–2490.
[38] A. Chatkon, P.B. Chatterjee, M.A. Sedgwick, K.J. Haller, D.C. Crans, Counterion affects interaction with interfaces: the antidiabetic drugs metformin and Decavanadate, Eur. J. Inorg. Chem. 2013 (10–11) (2013) 1859–1868.
[39] S. Treviño, D. Velázquez-Vázquez, E. Sánchez-Lara, A. Diaz-Fonseca, J.Á. Flores-Hernandez, A. Pérez-Benítez, et al., Metforminium decavanadate as a potential Metallopharmaceutical drug for the treatment of diabetes mellitus, Oxidative Med. Cell. Longev. 2016 (2016) 6058705.
[40] I. Sánchez-Lombardo, E. Sánchez-Lara, A. Pérez-Benítez, Á. Mendoza, S. Bernès, E. González-Vergara, Synthesis of Metforminium(2+) Decavanadates – crystal structures and solid-state characterization, Eur. J. Inorg. Chem. 2014 (27) (2014) 4581–4588.
[41] E. Sánchez-Lara, S. Treviño, B.L. Sánchez-Gaytán, E. Sánchez-Mora, M. Eugenia Castro, F.J. Meléndez-Bustamante, et al., Decavanadate salts of cytosine and metformin: a combined experimental-theoretical study of potential Metallodrugs against diabetes and Cancer, Front Chem. 6 (2018) 402.
[42] S. Treviño, E. Sánchez-Lara, V.E. Sarmiento-Ortega, I. Sánchez-Lombardo, J.Á. Flores-Hernández, A. Pérez-Benítez, et al., Hypoglycemic, lipid-lowering and metabolic regulation activities of metforminium decavanadate (H2Metf)3 [V10O28]·8H2O using hypercaloric-induced carbohydrate and lipid deregulation in Wistar rats as biological model, J. Inorg. Biochem. 147 (2015) 85–92.
[43] G. Fraqueza, L.A.E. Batista de Carvalho, M.P.M. Marques, L. Maia, C.A. Ohlin, W. H. Casey, et al., Decavanadate, decaniobate, tungstate and molybdate interactions with sarcoplasmic reticulum Ca2+-ATPase: quercetin prevents cysteine oxidation by vanadate but does not reverse ATPase inhibition, Dalton Trans. 41 (41) (2012) 12749.
[44] D. Marques-da-Silva, G. Fraqueza, R. Lagoa, A.A. Vannathan, S.S. Mal, M. Aureliano, Polyoxovanadate inhibition of *Escherichia coli* growth shows a reverse correlation with ca 2+ -ATPase inhibition, New J. Chem. 43 (45) (2019) 17577–17587.
[45] A.M. Silva-Nolasco, L. Camacho, R.O. Saavedra-Díaz, O. Hernández-Abreu, I. E. León, I. Sánchez-Lombardo, Kinetic studies of sodium and Metforminium Decavanadates decomposition and in vitro cytotoxicity and insulin- like activity, Inorganics. 8 (12) (2020) 67.
[46] M. Aureliano, F. Henao, T. Tiago, R.O. Duarte, J.J.G. Moura, B. Baruah, et al., Sarcoplasmic reticulum calcium ATPase is inhibited by organic vanadium coordination compounds: Pyridine-2,6-dicarboxylatodioxovanadium(V), BMOV, and an Amavadine analogue, Inorg. Chem. 47 (13) (2008) 5677–5684.
[47] M. Bradford, A rapid and sensitive method for the quantitation of microgram quantities of protein utilizing the principle of protein-dye binding, Anal. Biochem. 72 (1–2) (1976) 248–254.
[48] G. Fraqueza, C.A. Ohlin, W.H. Casey, M. Aureliano, Sarcoplasmic reticulum calcium ATPase interactions with decaniobate, decavanadate, vanadate, tungstate and molybdate, J. Inorg. Biochem. 107 (1) (2012) 82–89.
[49] M. Berrocal, J.J. Cordoba-Granados, S.A.C. Carabineiro, C. Gutierrez-Merino, M. Aureliano, A.M. Mata, Gold compounds inhibit the Ca2+-ATPase activity of brain PMCA and human neuroblastoma SH-SY5Y cells and decrease cell viability, Metals (Basel). 11 (12) (2021) 1934.
[50] T. Mosmann, Rapid colorimetric assay for cellular growth and survival: application to proliferation and cytotoxicity assays, J. Immunol. Methods 65 (1–2) (1983) 55–63.
[51] W. Strober, Trypan blue exclusion test of cell viability, Curr. Protoc. Immunol. 111 (2015). A3.B.1-A3.B.3.
[52] J. Schindelin, I. Arganda-Carreras, E. Frise, V. Kaynig, M. Longair, T. Pietzsch, et al., Fiji: an open-source platform for biological-image analysis, Nat. Methods 9 (7) (2012) 676–682.
[53] S. Treviño, E. González-Vergara, Metformin-decavanadate treatment ameliorates hyperglycemia and redox balance of the liver and muscle in a rat model of alloxan-induced diabetes, New J. Chem. 43 (45) (2019) 17850–17862.
[54] S. Meloche, J. Pouysségur, The ERK1/2 mitogen-activated protein kinase pathway as a master regulator of the G1- to S-phase transition, Oncogene. 26 (22) (2007) 3227–3239.
[55] V. Nogueira, Y. Park, C.-C. Chen, P.-Z. Xu, M.-L. Chen, I. Tonic, et al., Akt determines replicative senescence and oxidative or oncogenic premature senescence and sensitizes cells to oxidative apoptosis, Cancer Cell 14 (6) (2008) 458–470.
[56] E. Irving, A. Stoker, Vanadium compounds as PTP inhibitors, Molecules. 22 (12) (2017) 2269.
[57] M. Suganuma, H. Fujiki, H. Furuya-Suguri, S. Yoshizawa, S. Yasumoto, Y. Kato, et al., Calyculin a, an inhibitor of protein phosphatases, a potent tumor promoter on CD-1 mouse skin, Cancer Res. 50 (12) (1990) 3521–3525.
[58] D.R. Alessi, S.R. James, C.P. Downes, A.B. Holmes, P.R.J. Gaffney, C.B. Reese, et al., Characterization of a 3-phosphoinositide-dependent protein kinase which phosphorylates and activates protein kinase Bα, Curr. Biol. 7 (4) (1997) 261–269.
[59] R.J. Shaw, L.C. Cantley, Ras, PI(3)K and mTOR signalling controls tumour cell growth, Nature. 441 (7092) (2006) 424–430.
[60] A. Bijelic, M. Aureliano, A. Rompel, The antibacterial activity of polyoxometalates: structures, antibiotic effects and future perspectives, Chem. Commun. (Camb.) 54 (10) (2018) 1153–1169.
[61] M.B. Čolović, M. Lacković, J. Lalatović, A.S. Mougharbel, U. Kortz, D.Z. Krstić, Polyoxometalates in biomedicine: update and overview, Curr. Med. Chem. 27 (3) (2020) 362–379.
[62] N.I. Gumerova, A. Rompel, Polyoxometalates in solution: speciation under spotlight, Chem. Soc. Rev. 49 (21) (2020) 7568–7601.
[63] F. Zhai, X. Wang, D. Li, H. Zhang, R. Li, L. Song, Synthesis and biological evaluation of decavanadate Na4Co(H2O)6V10O28·18H2O, Biomed. Pharmacother. 63 (1) (2009) 51–55.
[64] M. Aureliano, C.A. Ohlin, M.O. Vieira, M.P.M. Marques, W.H. Casey, L.A.E. Batista de Carvalho, Characterization of decavanadate and decaniobate solutions by Raman spectroscopy, Dalton Trans. 45 (17) (2016) 7391–7399.
[65] L. Yatime, M.J. Buch-Pedersen, M. Musgaard, J.P. Morth, A.-M.L. Winther, B. P. Pedersen, et al., P-type ATPases as drug targets: tools for medicine and science, Biochim. Biophys. Acta Bioenerg. 1787 (4) (2009) 207–220.
[66] S. Ramos, M. Manuel, T. Tiago, R. Duarte, J. Martins, C. Gutiérrez-Merino, et al., Decavanadate interactions with actin: inhibition of G-actin polymerization and stabilization of decameric vanadate, J. Inorg. Biochem. 100 (11) (2006) 1734–1743.
[67] R. Xing, F. Wang, L. Dong, A.-P. Zheng, L. Wang, W.-J. Su, et al., Inhibitory effects of Na7PMo11CuO40 on mushroom tyrosinase and melanin formation and its antimicrobial activities, Food Chem. 197 (2016) 205–211.
[68] I.M. Gabas, G. Stepien, M. Moros, S.G. Mitchell, J.M. de la Fuente, In vitro cell cytotoxicity profile and morphological response to polyoxometalate-stabilised gold nanoparticles, New J. Chem. 40 (2) (2016) 1039–1047.
[69] F.J.C. Rossotti, H. Rossotti, Isopolyvanadates in acidic solution, J. Inorg. Nucl. Chem. 2 (3) (1956) 201–202.
[70] F. Corigliano, S. Di Pasquale, Decavanadate protonation degrees in aqueous solution, Inorg. Chim. Acta 12 (1) (1975) 102–104.
[71] A. Levina, A.I. McLeod, A. Pulte, J.B. Aitken, P.A. Lay, Biotransformations of antidiabetic vanadium prodrugs in mammalian cells and cell culture media: a XANES spectroscopic study, Inorg. Chem. 54 (14) (2015) 6707–6718.
[72] S.S. Soares, F. Henao, M. Aureliano, C. Gutiérrez-Merino, Vanadate induces necrotic death in neonatal rat cardiomyocytes through mitochondrial membrane depolarization, Chem. Res. Toxicol. 21 (3) (2008) 607–618.
[73] R.M.C. Gândara, S.S. Soares, H. Martins, C. Gutiérrez-Merino, M. Aureliano, Vanadate oligomers: in vivo effects in hepatic vanadium accumulation and stress markers, J. Inorg. Biochem. 99 (5) (2005) 1238–1244.
[74] S.S. Soares, C. Gutiérrez-Merino, M. Aureliano, Decavanadate induces mitochondrial membrane depolarization and inhibits oxygen consumption, J. Inorg. Biochem. 101 (5) (2007) 789–796.
[75] R. Sever, J.S. Brugge, Signal transduction in cancer, Cold Spring Harb. Perspect Med. 5 (4) (2015).
[76] W. Zhang, H.T. Liu, MAPK signal pathways in the regulation of cell proliferation in mammalian cells, Cell Res. 12 (1) (2002) 9–18.
[77] J.-X. Wu, Y.-H. Hong, X.-G. Yang, Bis(acetylacetonato)-oxidovanadium(IV) and sodium metavanadate inhibit cell proliferation via ROS-induced sustained MAPK/ERK activation but with elevated AKT activity in human pancreatic cancer AsPC-1 cells, J. Biol. Inorg. Chem. 21 (8) (2016) 919–929.
[78] Y. Fu, Q. Wang, X.-G. Yang, X.-D. Yang, K. Wang, Vanadyl bisacetylacetonate induced G1/S cell cycle arrest via high-intensity ERK phosphorylation in HepG2 cells, J. Biol. Inorg. Chem. 13 (6) (2008) 1001–1009.
[79] J. Rivadeneira, D.A. Barrio, S.B. Etcheverry, E.J. Baran, Spectroscopic characterization of a VO2+ complex of oxodiacetic acid and its bioactivity on osteoblast-like cells in culture, Biol. Trace Elem. Res. 118 (2) (2007) 159–166.
[80] J. Rivadeneira, A.L. Di Virgilio, D.A. Barrio, C.I. Muglia, L. Bruzzone, S. B. Etcheverry, Cytotoxicity of a vanadyl(IV) complex with a multidentate oxygen donor in osteoblast cell lines in culture, Med. Chem. 6 (1) (2010) 9–23.
[81] E. Bellomo, K. Birla Singh, A. Massarotti, C. Hogstrand, W. Maret, The metal face of protein tyrosine phosphatase 1B, Coord. Chem. Rev. 327–328 (2016) 70–83.
[82] M. Tolomeo, A. Cascio, The multifaced role of STAT3 in cancer and its implication for anticancer therapy, Int. J. Mol. Sci. 22 (2) (2021) 603.
[83] F. D'Onofrio, M.Q.U. Le, J.-L. Chiasson, A.K. Srivastava, Activation of mitogen activated protein (MAP) kinases by vanadate is independent of insulin receptor autophosphorylation, FEBS Lett. 340 (3) (1994) 269–275.
[84] K. Satyamoorthy, G. Li, M.R. Gerrero, M.S. Brose, P. Volpe, B.L. Weber, et al., Constitutive mitogen-activated protein kinase activation in melanoma is mediated by both BRAF mutations and autocrine growth factor stimulation, Cancer Res. 63 (4) (2003) 756–759.
[85] Q. Wang, T.-T. Liu, Y. Fu, K. Wang, X.-G. Yang, Vanadium compounds discriminate hepatoma and normal hepatic cells by differential regulation of reactive oxygen species, J. Biol. Inorg. Chem. 15 (7) (2010) 1087–1097.
[86] S. Markopoulou, E. Kontargiris, C. Batsi, T. Tzavaras, I. Trougakos, D.A. Boothman, et al., Vanadium-induced apoptosis of HaCaT cells is mediated by c-fos and involves nuclear accumulation of clusterin, FEBS J. 276 (14) (2009) 3784–3799.

[87] Y.-T. Li, C.-Y. Zhu, Z.-Y. Wu, M. Jiang, C.-W. Yan, Synthesis, crystal structures and anticancer activities of two decavanadate compounds, Transit. Met. Chem. 35 (5) (2010) 597–603.
[88] H. El Moll, W. Zhu, E. Oldfield, L.M. Rodriguez-Albelo, P. Mialane, J. Marrot, et al., Polyoxometalates functionalized by bisphosphonate ligands: synthesis, structural, magnetic, and spectroscopic characterizations and activity on tumor cell lines, Inorg. Chem. 51 (14) (2012) 7921–7931.
[89] M. Cheng, N. Li, N. Wang, K. Hu, Z. Xiao, P. Wu, et al., Synthesis, structure and antitumor studies of a novel decavanadate complex with a wavelike two-dimensional network, Polyhedron. 155 (2018) 313–319.